

Turbidity Maximum and Secondary Flow in a Cross-section of a Meandering Estuary: Chikugo River, Japan

Katuhide Yokoyama¹, Yu Kaneko² and Kouichi Yamamoto³

¹Department of Civil and Environmental Engineering
Tokyo Metropolitan University
1-1 Minamiosawa, Hachioji, Tokyo, 192-0397
JAPAN

²Yachiyo Engineering Co., Ltd.
2-18-12 Nishiochiai, Shinjuku, Tokyo, 161-8575
JAPAN

³Department of Civil and Environmental Engineering
Yamaguchi University
2-16-1 Tokiwadai, Ube, Yamaguchi, 755-8611
JAPAN

E-mail: k-yoko@tmu.ac.jp

Abstract: *The influence of a meander on a cross-sectional distribution of turbidity maximum was investigated by vessel-mounted ADCP in the estuarine channel of the Chikugo river. The along-river current was relatively weak at the inside of the curve and was strong at the outside of the curve during flood tide. The cross-channel currents near the bottom flowed from the outside to the inside of the curve, and the suspended sediment concentration was high at the inside of the curve. These facts suggest that the secondary current occur in the meander of tidal channel and the suspended sediment transported by the turbidity maximum is moved into the inside of the bend. A fluid mud layer with a maximum velocity of 0.4 m/s was formed at the inside of the curve. The maximum thickness of the mud layer increased to 1.2 m during a flood tide, and it remained 0.1 m after one tidal cycle.*

Keywords: *meander, estuary, turbidity maximum, secondary current, fluid mud, ADCP*

1. INTRODUCTION

Meandering channel is formed in alluvial plane by erosion of the outer banks and deposition of bed-load on the inner banks. The migration of meander bend was examined geomorphologically (e.g., Hudson and Kesel, 2000). The stream flow and sediment dynamics in meander bends were investigated both theoretically and experimentally (Quick, 1974; Ikeda, 1982). Recently, advanced numerical model of river morphology have been proposed, Darby *et al.* (2002) developed two-dimensional numerical simulation of bank erosion and channel migration in meandering rivers and Olsen (2003) used three-dimensional CFD model to compute the formation of the meandering pattern in an initially straight alluvial channel.

At actual river bend, Bathurst *et al.* (1979) successfully measured the pattern of secondary circulation using electromagnetic current meter. Since the 1990s, many researchers have used acoustic Doppler current profiler (ADCP) to measure the river flow, and detailed secondary circulation pattern was presented (Richardson and Thorne, 1998; Dinehart and Burau, 2005; Fong *et al.*, 2009).

However, few studies have investigated the relationship between formation of curving channel and flow field in an estuary. Yokoyama *et al.* (2011) calculated annual sediment budget in a river mouth estuary and demonstrated that the suspended sediment transport by estuarine turbidity maximum significantly affect to the topography of tidal flat and estuarine channel, but they did not refer to the lateral sediment transport and the change in a cross-sectional bed topography. Blanton *et al.* (2003) describes the transport of salt and suspended sediments in a curving channel of an estuary, but lateral variation of suspended sediment and current distribution in a cross section were not measured. This paper focuses on the secondary circulation and the transport of suspended sediments in a cross section of curving channel of the Chikugo River estuary.

2. STUDY SITE

The Chikugo river is situated in western Japan, and dominates discharges into the Ariake Sea. The Chikugo river ranks as the 22nd largest river in Japan, with a drainage basin of 2,860 km², a total length of 143 km, a mean discharge of 54 m³/s during dry season, and a mean annual storm discharge of 2,800 m³/s. The tidal limit of the Chikugo river occurs at the barrage, which is 23 km upstream from the river mouth (Fig. 1). The estuarine channel has continuous mild meander with a radius of curvature of 1.5 – 3 km, and the channel width varies from 1,000m at the river mouth to 250 m at the barrage.

The tidal range is 5 m at spring tide and 1.5 m at neap tide. The estuary is classified as well-mixed on account of the large tidal range at the mouth. Strong tidal currents occur in the estuary, the surface velocity increases over 1 m/s. The suspended sediment concentration (SSC) within estuarine turbidity maximum zone (ETM) is 20 –100 mg/l at neap tide, and 1,000 – 3,000 mg/l at spring tide, which is the highest concentration in Japan. The bottom sediments in the section between the river mouth (0 km) and 8 km consist mainly of fine sand, the mud contents of the sediments increases towards upstream. The maximum mud contents (98 %) are found at a distance of 14 –16 km from the river mouth, the region is corresponding to the ETM front.

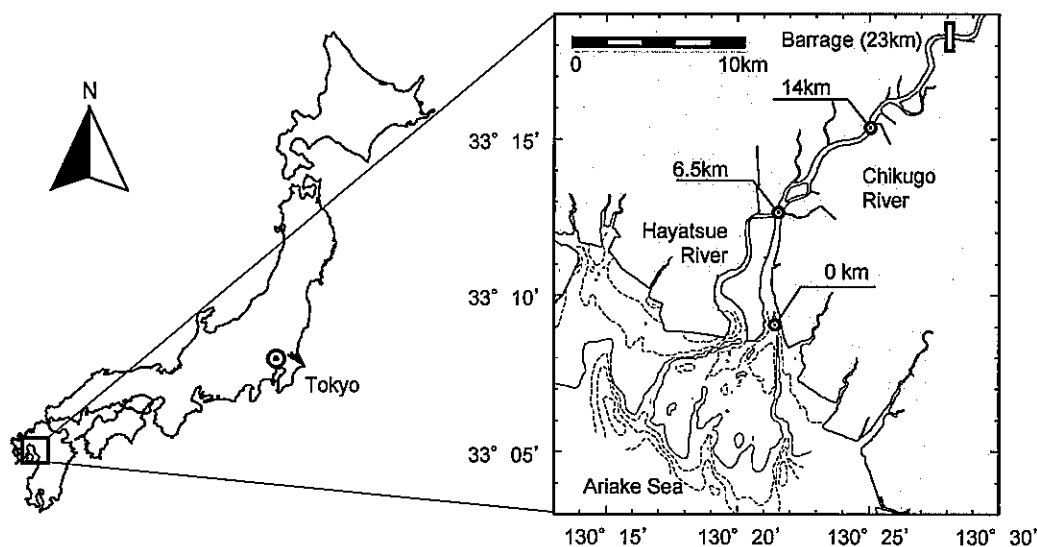


Figure 1 Location of the Chikugo River

3. MATERIALS AND METHODS

Data of water velocity, salinity and the SSC were collected in August 31, 2007 at the cross-section 14 km from the river mouth, that locates upstream of channel curve (Figure 2(a)). The river bed material is soft mud in winter (water content is approximately 200%), and the mud is flushed away by storm runoff occurred in June – July, whereas after consolidated mud or sand layer appear every year. Field observations were undertaken in the eroded cross-section (Figure 2(b), thick solid line) during spring tides, and the maximum depths at the transect was 2.8 m at low tide (7:00), 7.8m at high tide (11:20), 2.7 m at low tide (19:20). Freshwater inflow was 75 m³/s during the fieldwork period.

Velocity profiles in the cross section were measured using a 1,200 kHz acoustic Doppler current profiler (Workhorse Sentinel 1,200 kHz, Teledyne RDI). The vertical bin size was set to 0.25 m and the first cell-range from the water surface was 0.57 m, and the ensemble interval was approximately 3 seconds. ADCP was mounted on the side of the boat, the speed of boat cruise was 5 km/h. Vertical profiles of salinity and SSC were measured using CTD with optical backscatter sensor (AAQ-1183, JFE Advantech) at five stations in the return cruise. It took 10 – 15 minutes for one round cruise, and ADCP-OBS measurements along the transect were conducted every 20 minutes over one tidal cycle (12.5 hour).

The uncertainty of collected velocity profiles were verified using the fixed ADCP data. A moving boat ADCP determines water velocity over the ground by the combination of relative water velocity and boat speed. Boat speed was processed using both bottom track data and DGPS data, and bottom track data will be biased when channel sediment moves. A downward looking ADCP (Aquadopp 1 MHz, Nortek AS) was mounted on the bottom of a FRP twin hull catamaran of 1.2 m long, and the boat was anchored at the position between station C and station D. The bin size was set to 0.4 m and the first cell range from top of the water was 0.3 m, the average interval was 5 seconds.

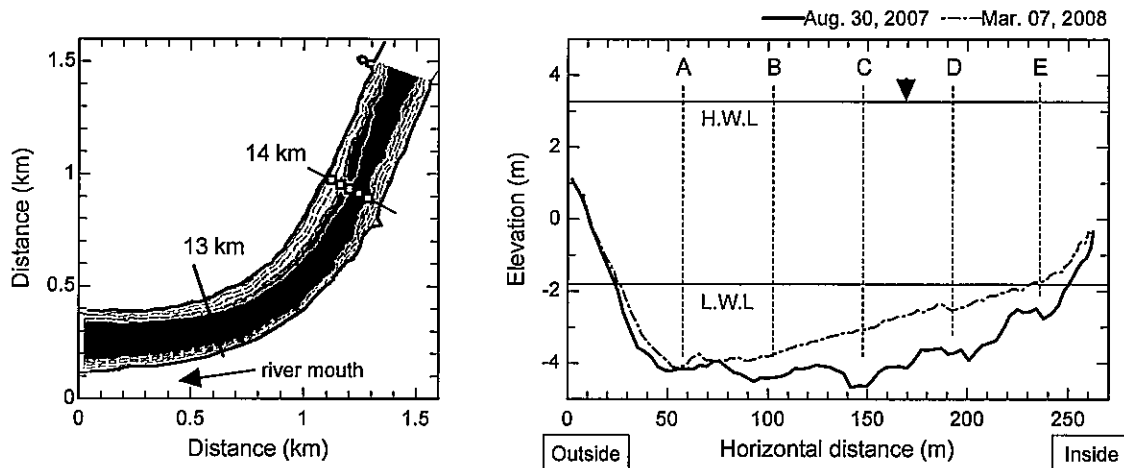


Figure 2 (a) Bathymetry of the measurement location, and (b) cross-section of the transect located 14 km from the river mouth. (b) The thick solid line denotes the eroded channel bed immediately after the storm discharge, and the thin line denotes the deposited bed half a year after the flood. The vertical dotted line and the triangular mark indicate, respectively, positions at which salinity and SSC were measured, and ADCP was moored downward.

4. RESULTS

The lateral distributions of velocity in the stream cross-section are shown in Figure 3, looking downstream. The left bank shown in Figure 3 corresponds to the outside of the bends (southeast bank) shown in Figure 2(a). Along channel velocity was determined using DGPS information as the boat velocity reference, and cross channel velocity was determined using bottom track data. The bottom track often lost the contact to the channel bed due to low density mud, while the accuracy of processed velocity is high. Salinity in the measurement cross section was uniform either laterally or vertically, and the value was 0 psu at low tide and increased to 0.5 psu at high tide.

The along-channel currents during flood tide (Figure 3(a)) was asymmetry, strongest at the left side of the channel (outside of the bend), the maximum landward velocity exceeded 1.3 m/s. The cross-channel currents (Figure 3(b)) shows that the surface water flowed from the inside to the outside of the curving channel, and the bottom water flowed in the opposite direction, the maximum velocity at water surface and at near bottom reached 0.15 m/s respectively. These current patterns show that secondary currents occurred during flood tide.

On the other hand, the along channel currents during ebb tide (Figure 3(c)) was strongest at the center of the channel. The cross-channel current (Figure 3(d)) was very weak, the average value of the absolute velocity was 0.025 m/s, the tendency of flow pattern was not found. Therefore, symmetric open channel flow occurred in the cross section.

The vertical profiles of SSC measured in five stations were shown in Figure 4. SSC at the outside of the bend (station A) were uniform vertically, the depth averaged concentration was 500 mg/l. At the inside of the bend (station D), the surface SSC was approximately 300 mg/l and the maximum SSC near bottom reached 4,000 mg/l, that is the upper limit of the OBS sensor. It is assumed that SSC just above the bottom exceeded 4,000 mg/l and fluid mud appeared on the bottom, though the value of SSC reduced rapidly due to sensor saturation.

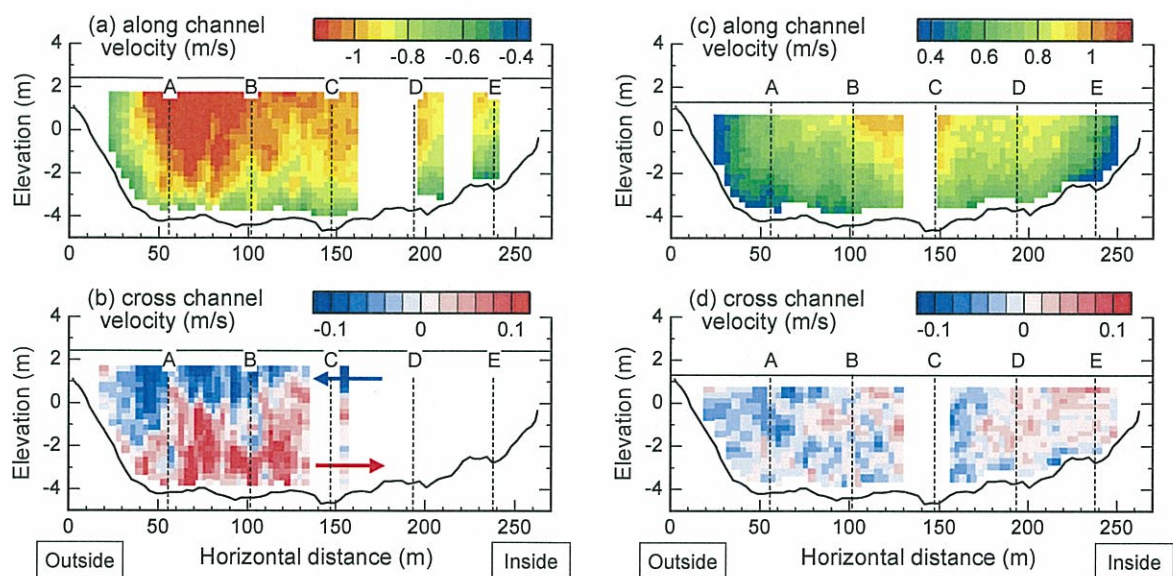


Figure 3 Current distributions in the cross section of curving channel; (a) along channel velocity and (b) cross channel velocity during flood tide, (c) along channel velocity and (d) cross channel velocity during ebb tide.

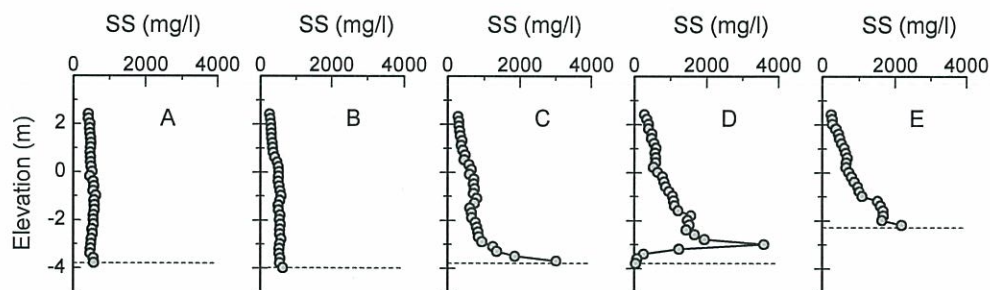


Figure 4 Vertical profiles of suspended sediment concentration during flood tide

5. DISCUSSION

5.1. Secondary flow and suspended sediment transport

Secondary flow occurred in the measurement cross-section during flood tide, whereas it was not found during ebb tide. The measurement cross-section is not located at the middle part of the bend, is located at the joint of curve section and straight section of the river channel (Figure 2a). The transect section corresponds to the exit of curving channel and the entrance of straight channel when saline water advect from the river mouth, on the other hand, river water run through the transect section as a exit of straight channel when fresh water flow downstream. Therefore, secondary current occur at the measurement cross-section when sea water intrude into the estuary during flood tide, and normal symmetric open channel flow occur when river water move downstream during ebb tide.

Lateral SSC distribution shown in Figure 4 increased from the inside to the outside of the bend at the water surface, and it extremely increased from outside to the inside near the bed. In general, the suspended sediment concentration is almost uniform vertically when turbid water including silt and clay run through middle reach of a river by a storm runoff. The SSC distribution and flow pattern indicates that the suspended particle is carried outward at the water surface and inward near the

bottom by secondary circulation. Moreover, suspended particles are flocculated into large particles and settled rapidly at the inside of the bend because water current becomes weak and turbulence intensity decreases.

5.2. Fluid mud movement

When strong tidal current that exceeded 0.5 m/s occurred, the bottom-referenced velocity profile was different from the GPS-referenced velocity profile. The bottom-referenced velocity profile moved from the GPS-referenced velocity profile in parallel, and the latter was almost equal to the velocity measured with moored ADCP (Figure 5(a)). It is recognized that the water velocity referencing the GPS data shows a true value, and the difference in the velocity determined by two methods shows the speed of the moving bed.

The lateral variations of depth averaged velocity determined by two methods (Figure 5(b)) were equal at the outside of the bend (around station A, B), this good agreement between two values indicate that the channel bed was stable. However, the velocity referencing bottom tracking data decreased unnaturally at the inside of the bend (around station C, D). It is suggested that fluid mud existed on the inner bend and migrated upstream or downstream. Bottom sediment at inner bend begun to move upstream when the depth averaged velocity exceeded 0.5 m/s during flood tide, and the maximum migration speed of 0.4 m/s was observed. It stopped at slack high tide, they reversed the direction of migration to the river mouth during ebb tide.

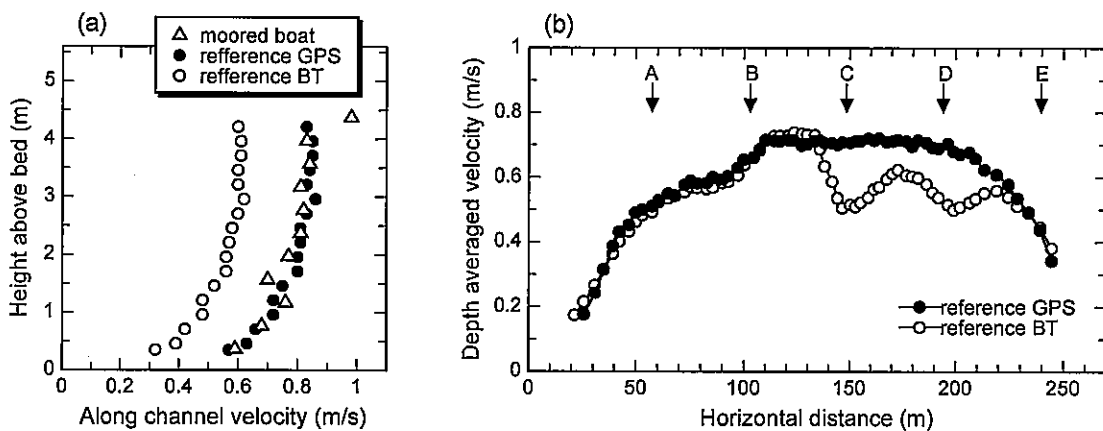


Figure 5 Comparison of velocity, (a) vertical profiles measured from moored boat and moving boat, (b) lateral distribution of depth averaged velocity processed using GPS information and bottom track data of ADCP.

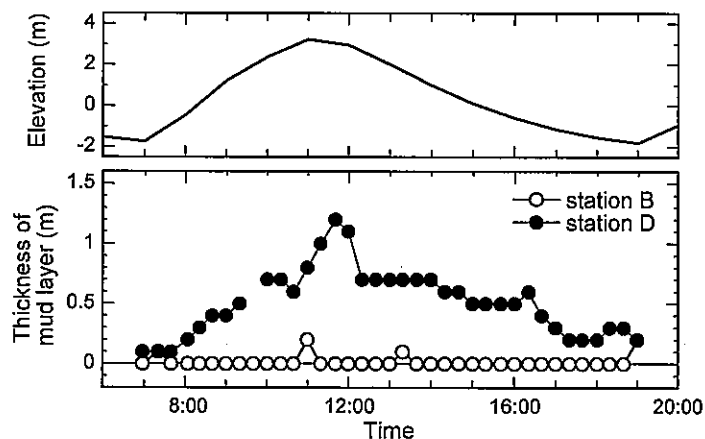


Figure 6 Time series of water level and fluid mud thickness

The thickness of fluid mud was estimated using SSC profile of each measurement station (Figure 6). Fluid mud was not found at the station B, positioned at outside of the curve, while evolution of the fluid mud thickness was found at station D, positioned at inside of the curve. The thickness at inner bend increased during flood tide and the maximum thickness of 1.2 m was observed at slack high tide. Thereafter, fluid mud reduced the thickness during ebb tide. The thickness was 0.1 m at the first low tide, and it became 0.2 m at the next low tide, therefore the net aggradation of channel bed was 0.1 m during one semi-diurnal tide.

Suspended sediment deposit on the inside of a bend due to both inward sediment transport by secondary circulation and increase in settling velocity by flocculation, and they form fluid mud. Fluid mud migrates upstream and downstream with tidal currents, and the river bed elevation of inner bend increases. The muddy point bar has appeared upstream region of the curve (Figure 2(a)), this morphological feature suggests that the net transport of fine sediment is up-estuary.

6. CONCLUSION

Estuarine turbidity maximum moved in the meandering Chikugo River estuary, and secondary circulation developed when the ETM flowed through the curving channel. Suspended sediment moved outer bend at the water surface and inner bend near the bottom. Moreover, flocculation of fine particles would have occurred and the settling velocity would have increased because the water velocity became weak at the inside of the bend. As a result, suspended sediment concentration near the bottom increased extremely, and fluid mud formed on the river bed. Fluid mud migrated with strong tidal current, the thickness increased during flood tide and decreased during ebb tide. It is suggested that net sediment transport is up-estuary because the muddy point bar appears upstream of the curve.

7. REFERENCES

- Bathurst, J. C., Thorne, C. R. and Hey, R. D. (1979), *Secondary flow and shear stress at river bends*, J. Hydraulics Division, ASCE, 105(10), 1277-1295.
- Blanton, J. O., Seim, H., Alexander, C., Amft, J. and Kineke, G. (2003), *Transport of salt and suspended sediments in a curving channel of a coastal plain estuary: Satilla River, GA*, Estuarine, Coastal and Shelf Science, 57, 993-1006.
- Darby, S. E., Alabyan, A. M. and Van De Wiel, M.J. (2002), *Numerical simulation of bank erosion and channel migration in meandering rivers*, Water Resources Research, 38(9), 1163.
- Dinehart, R. L. and Burau, J. R. (2005), *Averaged indicators of secondary flow in repeated acoustic Doppler current profiler crossings of bends*, Water Resources Research, 41(9), W09405.1-18
- Fong, D. A., Monismith, S. G., Stacey, M.T. and Burau, J. R. (2009), *Turbulent stresses and secondary currents in a tidal-forced channel with significant curvature and asymmetric bed forms*, J. Hydraulic Engineering, ASCE, 135(3), 198-208.
- Hudson, P.F. and Kesel, R. H. (2000), *Channel migration and meander-bend curvature in the lower Mississippi River prior to major human modification*, Geology; 28(6), 531-534.
- Ikeda, S. (1982), *Lateral bed Load transport on side slopes*, J. Hydraulics Division, ASCE, 108(11), 1369-1373.
- Olsen, N. R. B. (2003), *Three-dimensional CFD modeling of self-forming meandering channel*, J. Hydraulic Engineering, ASCE, 129(5), 366-372.
- Quick, M. C. (1974), *Mechanism for streamflow meandering*, J. Hydraulics Division, ASCE, 100(6), 741-753.
- Richardson, W. R. and Thorne, C. R. (1998), *Secondary currents around braid bar in Brahmaputra River, Bangladesh*, J. Hydraulic Engineering, ASCE, 124(3), 325-328.
- Yokoyama, K., Suetsugi, T. and Kawano, K. (2011), *Annual sediment budget in the Shirakawa River estuary, Japan*, Christodoulou and Stamou (Eds) *6th International Symposium on Environmental Hydraulics, IAHR*, Greece, 893-898.